International Journal of Mechanical and Electrical Engineering
ISSN: 3005-9615 (Print), ISSN: 3005-7132 (Online) | Volume 8, Number 1, Year 2026
DOI: https://doi.org/10.62051/ijmee.v8n1.15
Journal homepage: https://wepub.org/index.php/IJMEE/index

Comprehensive Optimization Design for the A-Axis Support of an AC Double-Swing Angle Milling Head

Hailin Liao, Yun Xu *, Tao Zhang, Wenlu Zhang

College of Mechanical Engineering, Sichuan University of Science & Engineering, Yibin, Sichuan, P.R. China

* Corresponding Author: Yun Xu

ABSTRACT

As a critical component of the AC double-swing angle milling head, the A-axis support significantly influences its dynamic and static performance. To reduce its mass while meeting static and dynamic requirements, systematically optimize the A-axis support structure, enhance the operational performance of the milling head, and lower material costs, a method combining topology optimization and multi-objective optimization is proposed. The original static and dynamic performance of the A-axis support is analyzed, and optimization objectives are defined. Topology optimization is then employed to identify optimizable regions of the A-axis support, based on which the structure is reconstructed.Based on the topology optimization results, a mathematical model is established with design variables including the wall thickness, rib thickness, and lightening hole size of the A-axis support. The optimization objectives are to minimize mass and maximize the first-order natural frequency, with deformation as the constraint. The Central Composite Design (CCD) method is used to obtain initial sample points, a Kriging model is constructed to establish the response surface, and finally, the Multi-Objective Genetic Algorithm (MOGA) is applied for optimization. After optimization, the deformation of the A-axis support is less than before, meeting the static stiffness requirement. The mass is reduced by 13.87%, achieving the lightweight objective, and the total deformation is decreased by 22.1%, indicating improved static performance.

KEYWORDS

AC Double-Swing Angle Milling Head; A-Axis Support; Multi-Objective Optimization; Lightweight Design.

1. INTRODUCTION

Industrial strength is a crucial reflection of a country's overall power. Enhancing the capability of the equipment manufacturing industry serves as an important prerequisite for building an industrial powerhouse and a key link in narrowing the gap with developed countries. This is particularly vital for nations still in the early stages of industrialization [1]. In the process of advancing the equipment manufacturing industry, the development of CNC machine tools is indispensable. As the "mother machine" of industry, CNC machine tools directly influence the development level of several key sectors, including aerospace, automotive, and shipbuilding. The dual-axis milling head, being a core component of large five-axis CNC machine tools, has its precision directly affecting the overall machining performance of the machine [2-4].

With the rapid advancement of modern machine tool technology, dual-swing angle CNC milling heads are gaining widespread application [5]. In high-precision machining fields such as aerospace, medical, and military industries, these milling heads can achieve the machining of high-quality

workpieces, demonstrating their irreplaceable process advantages [6]. The performance of dual-swing angle CNC milling heads has become a significant indicator for measuring the technical level of CNC machine tools. Against the backdrop of rapid industrial technological iteration, the market is imposing higher demands on the performance of dual-swing angle milling heads: on one hand, they require higher stability and precision when machining high-precision, difficult-to-machine parts, and positioning deviations must be strictly controlled; on the other hand, greater torque output is needed for machining large workpieces. Traditional machine tool milling heads can no longer adequately meet these escalating demands, leading to an expanding application scope for dual-swing angle CNC milling heads [7], as shown in Figure 1.

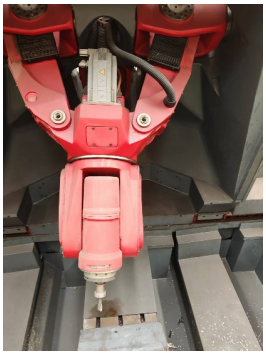

Figure 1. AC Double-Swing Angle Milling Head

2. FINITE ELEMENT ANALYSIS OF THE A-AXIS SUPPORT

2.1. Establishment of the Finite Element Model

Based on the two-dimensional drawings provided by the company, three-dimensional modeling was performed using SOLIDWORKS software. The AC double-swing angle milling head consists of the C-axis housing, C-axis torque motor, YRT bearings, A-axis housing, A-axis torque motor, spindle housing, spindle, encoder, and other components. When establishing the finite element model of the double-swing angle milling head, in order to control the mesh count and reduce the computational load, it is necessary to simplify the model while fully capturing the structural mechanical characteristics [8]. The simplified model is shown in Figure 2 below.

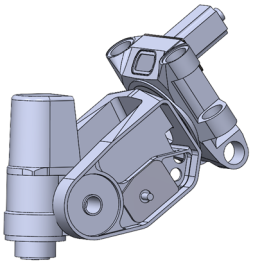

Figure 2. Simplified Model of the A/C Double-Swing Angle Milling Head

Table 1. Material Properties

Component	Spindle Housing, A-axis Housing, C-axis Housing	Others
Material	QT600-3	45#stel
Density (kg/m³)	7850	7890
Elastic Modulus (GPa)	200	209
Poisson's Ratio	0.3	0.269

2.2. Load Calculation

Since the experimental simulation involves a fixed-position condition for the AC double-swing angle milling head components, to further increase simulation analysis speed, the connection points between the AC double-swing angle milling head and the main machine body can be set as fixed constraints, while the connections between other components utilize bonded contacts. The primary machining method for this AC double-swing angle milling head is milling; therefore, this paper focuses on calculating the load conditions on the milling head during milling operations.

During the milling process, the main loads borne by the AC double-swing angle milling head include milling forces and its own weight. Standard gravitational acceleration is applied to the entire milling head assembly, and the components of the milling force in three mutually perpendicular directions are applied at the spindle. When calculating with a high-speed steel tool and a carbon steel workpiece material, the empirical formula for the principal milling force is [9]:

$$F_c = C_{F_c} a_p f_z^{0.72} D^{-0.86} B^{0.86} Z K_{F_c} \tag{1}$$

Where：F_c is the milling force (N)； C_{F_c} is the milling force coefficient； a_p is the depth of cut (mm)； f_z is the feed per tooth (mm)； is the milling cutter diameter (mm)； B is the milling width (mm)； Z is the number of cutter teeth； K_{F_c} is the correction factor. where the correction factor K_{mF_c} 、 where the correction factor Kc can be obtained from the product of the material coefficient Km, the tool rake angle coefficient Kγ, and the tool lead angle coefficient Kφ, i.e., Kc = Km · Kγ · Kφ. The values for each coefficient in the formula can be obtained by consulting the relevant coefficient tables [10].

Based on actual conditions or reference tables, the values of the coefficients in Equation (1) are determined as: $C_{F_c} = 669$, $a_p = 1.8$, $f_z = 0.3$,D=10,B=10,Z=5. Substituting these values into Equation (1) yields the main milling force F_c :

$$F_c = 669 \times 1.8^{1.1} \times 0.3^{0.72} \times 10^{-0.86} \times 10^{0.86} \times 5 \times 0.73 \approx 1942 \tag{2}$$

In end milling, the magnitudes of the component forces in each direction can be calculated using the following formulas: the vertical component force $F_v = 0.5F_c = 971N$,lateral component force $F_e = 0.3F_c = 582.6N$, longitudinal component force $F_f = 0.9F_c = 1747.8N$,In actual machining, the milling force can vary significantly depending on the milling conditions [11].

2.3. Static Analysis

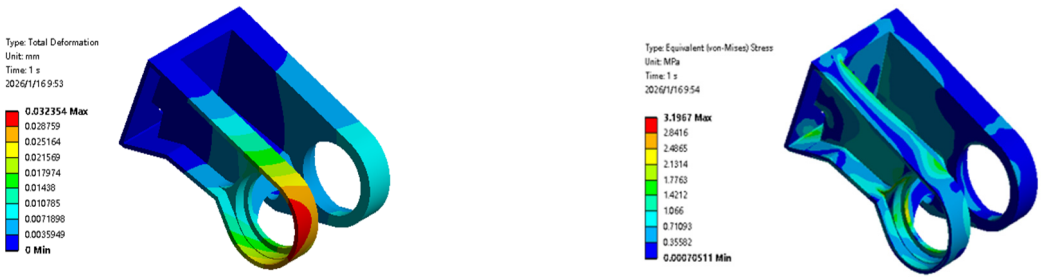

(a)Total Deformation of A-Axis Support (b)Stress on A-Axis Support

Figure 3. Contour Plots of Total Deformation and Stress on the A-Axis Support

Static mechanics serves as the foundation for conducting finite element analysis of model structures. Performing static analysis on the AC double-swing angle milling head enables the identification of areas where stress and deformation are most concentrated within the system, providing critical evidence for model optimization and improvement.

2.4. Modal Analysis

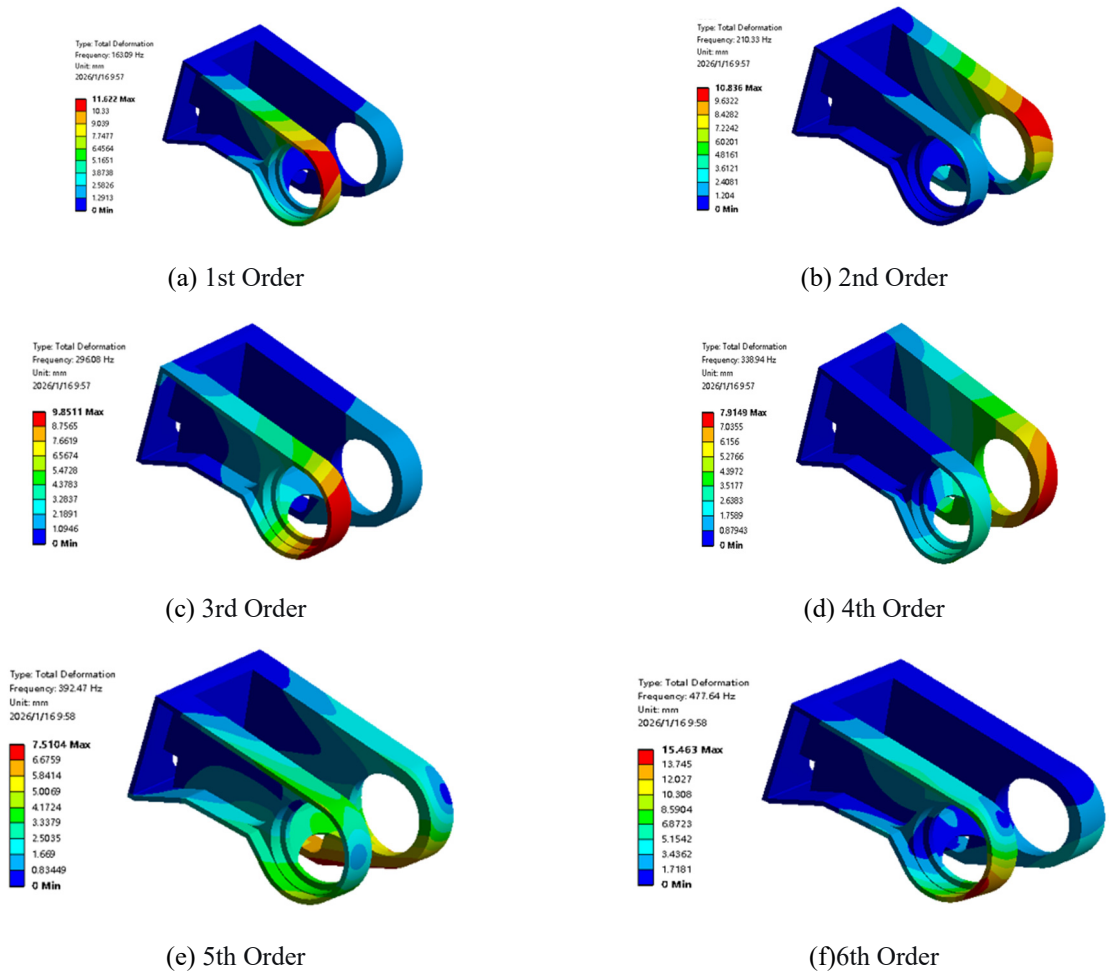

(a) 1st Order (b) 2nd Order

(c) 3rd Order (d) 4th Order

(e) 5th Order (f)6th Order

Figure 4. First Six Mode Shapes of the A-Axis Support

Table 2. Modal Analysis Results of the A-Axis Support

Order	Frequency/Hz	Mode Shape Description
1	163.09	Lower part of A-axis housing rotates counterclockwise around the Z-axis.
2	210.35	Left end of the lower A-axis housing stretches along the positive Y-direction, while the right end stretches along the negative Y-direction.
3	296.08	Lower part of A-axis housing stretches along the negative Z-direction.
4	338.92	Entire A-axis housing rotates clockwise around the X-axis.
5	392.47	Lower end of A-axis housing twists counterclockwise around the Z-axis.
6	477.65	Left end of the lower A-axis housing stretches along the negative Y-direction, while the right end stretches along the positive Y-direction.

As a component of the AC double-swing angle milling head, the A-axis housing is also the most susceptible structure to deformation. Therefore, analyzing its dynamic characteristics is essential. Its upper end is connected to the C-axis via bolts, and its lower end is connected to the A-axis via bolts. If its dynamic characteristics cannot be ensured, the precision of the spindle will be compromised.

When setting the fixed constraints for the A-axis housing, the same configuration as in the previous static analysis is maintained. Specifically, in ANSYS Workbench, the contact surface where the A-axis housing connects to the C-axis bolts is defined as a fixed constraint. The first six modes of the A-axis housing are solved as a reference. The resulting mode shapes for the first six modes are shown in Figure 4, and the corresponding natural frequencies and mode shape characteristics are listed in Table 2.

3. TOPOLOGY OPTIMIZATION AND STRUCTURAL REDESIGN OF A-AXIS SUPPORT

Topology optimization is a method that determines the optimal material distribution within a predefined design space by selectively removing material, based on specific objectives, constraints, loads, and boundary conditions [12]. This approach can provide valuable guidance for structural design. In this study, the structural optimization module in ANSYS Workbench is employed to optimize the A-axis support. Before optimization, the A-axis support is first filled to achieve a larger design space and better reflect its optimal structural layout. The filled model is shown in Figure 5, the topology-optimized structure in Figure 6, and the reconstructed model in Figure 7.

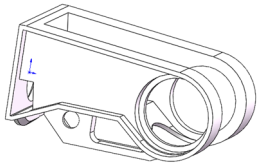

Figure 5. Filled Model

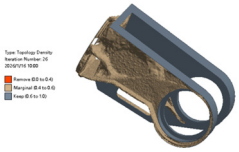

Figure 6. Topology Optimization Model

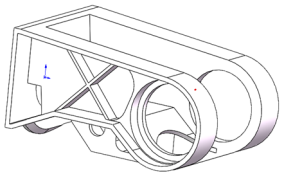

Figure 7. Reconstructed Model

4. MULTI-OBJECTIVE OPTIMIZATION DESIGN OF THE A-AXIS SUPPOR

4.1. Optimization Model Establishmen

Based on the structural characteristics of the selected A-axis housing, eight dimensions were initially identified as key parameters. The selected dimensions are illustrated in the figure below, where:n1 is the rib thickness,n2 is the thickness of the left and right end faces,n3 is the thickness of the left side plate,n4 is the thickness of the right side plate,n5 is the left side width,n6 is the right side width,n7 is the motor plate thickness,n8 is the thickness of the intermediate end face.The initial parameters of the A-axis housing are kept consistent with the original A-axis housing. The initial thickness of the A-axis housing ribs is set to 10 mm. According to the structural optimization design requirements, each parameter is allowed to vary by 10–15% above or below its initial value.

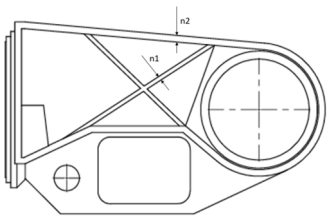

Figure 8. Two Design Parameters of the A-Axis Support (Left View)

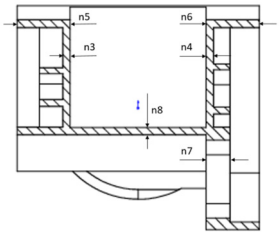

Figure 9. Six Design Parameters of the A-Axis Support (Frontal Section View)

In the previous section, the establishment of the structural optimization mathematical model has been introduced. Based on the preceding analysis results, it is evident that the current A-axis housing

demonstrates relatively weak stiffness performance, while the mass of the A-axis housing after adding ribs is slightly greater than that of the original design. Therefore, this study adopts stiffness maximization and mass minimization as the optimization objective functions, and selects the key dimensions of the A-axis housing as optimization variables. Simultaneously, to ensure that the dynamic performance of the A-axis housing meets design standards, the first-order natural frequency must be higher than that of the original A-axis housing. Accordingly, during the optimization process, the first-order natural frequency is set as a constraint condition to establish the multi-objective optimization mathematical model for the A-axis housing:

$$\begin{cases} D = \left(D_1, D_1, D_1, D_1, D_1, D_1, D_1\right)^T \\ Min\ \delta(D) \\ f(D) \geq f_0 \\ Min\ M(D) \\ s.t. D_{iL} \leq D_i \leq D_{iH} \end{cases} \tag{3}$$

Where: $D\ is$ represents the design variables of the A-axis housing (mm);$\delta(D)$is the total deformation (mm);$f(D)$ is the first-order natural frequency (Hz);$M(D)$ is the mass (kg);D_{iL} is the lower limit of the design variables; ;D_{iH} is the upper limit of the design variables.

Table 3. Ranges of Optimization Parameters

Parameter	**Initial Value**(mm)	**Variation Range**(mm)	**Parameter**	**Initial Value**(mm)	**Variation Range**(mm)
n_1	10	8.5-11.5	n_5	109	98-120
n_2	16	14.5-17.5	n_6	109	98-120
n_3	15	13.5-16.5	n_8	16	14.5-17.5
n_4	15	13.5-16.5			

4.2. Response Surface Establishment

In this study, 141 sets of key dimension combinations were generated through parametric sampling, and the corresponding deformation and first-order natural frequency of the A-axis support for each set were calculated using the finite element method. Based on this, Spearman's rank correlation analysis was employed to quantify the influence degree of each dimensional variable on the aforementioned performance indicators. The specific analysis results are shown in the figure below.

From the figure, it can be observed that n1, n2, n3, n4, n5, n6, and n8 have a significant impact on total deformation, while n1, n2, n3, n4, n5, n6, and n8 also significantly affect the first-order natural frequency. Therefore, based on the comprehensive analysis above, n1, n2, n3, n4, n5, n6, and n8 are selected as the seven key dimensional design variables for optimizing the A-axis housing structure.

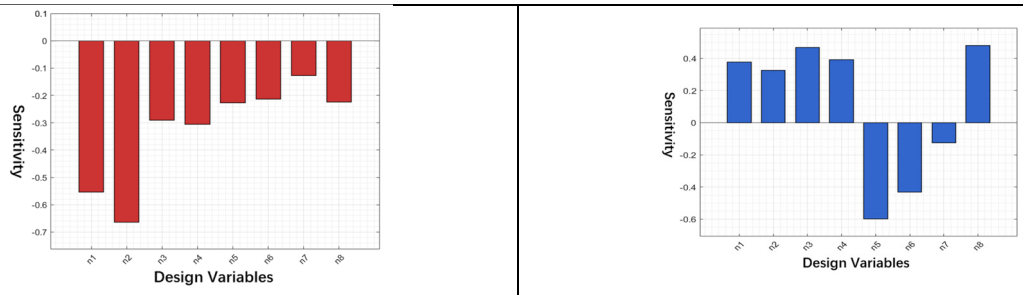

(a)**Total Deformation Sensitivity** (b)**Mass Sensitivity**

Figure 10. Sensitivity Analysis Diagram of A-Axis Support

4.3. Multi-Objective Optimization of A-Axis Support

The Multi-Objective Genetic Algorithm (MOGA) is an algorithm used to solve multi-objective optimization problems. By continuously performing selection, crossover, and mutation, it evolves the individuals within the population to search for Pareto optimal solutions in multi-objective optimization problems. Based on the aforementioned Kriging response surface model, optimization objectives, and constraint conditions, the target problem is solved to obtain the optimal solution set. After appropriate adjustments and rounding, the results are shown in Table 4.

Table 4. Parameter Optimization Results

Parameter	**values**
n_1(mm)	11
n_2(mm)	17.5
n_3(mm)	16.5
n_4(mm)	13.5
n_5(mm)	119.5
n_6(mm)	98.5
n_8(mm)	16.5

The contour plots of maximum deformation and stress for the A-axis support are shown in the figures below, and the first-order mode shape is also illustrated. Before optimization, the maximum deformation of the original A-axis housing was 0.032353 mm, the maximum principal stress was 3.229 MPa, and the first-order natural frequency was 163.09 Hz. After optimization, the maximum deformation of the A-axis housing decreased by 22.1%, the stress reduced by 7.1%, and the first-order natural frequency increased by approximately 11.3%.

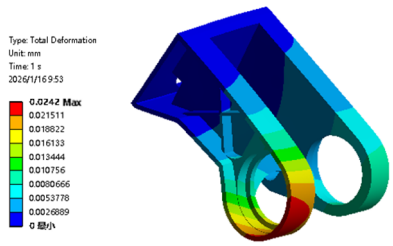

(a) Deformation Diagram

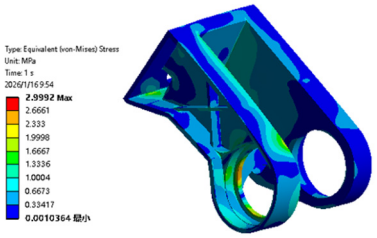

(b)Stress Contour Plot

Figure 11. Deformation and Stress Contour Plots of the Optimized A-Axis Support

5. CONCLUSION

This study employs a combined approach of topology optimization and multi-objective optimization to enhance the design of the AC double-swing angle milling head. The objectives are to reduce the mass and total deformation of the A-axis support while ensuring its static stiffness. The following conclusions are drawn:

(1) Through topology optimization, the optimizable regions of the A-axis support were identified, and the A-axis support model was reconstructed based on the topology optimization results.

(2) Using the Multi-Objective Genetic Algorithm (MOGA) for optimization, the deformation of the A-axis support after optimization is less than that before optimization, meeting the static stiffness requirements. The mass of the A-axis support is reduced by 13.87%, achieving the lightweight objective, while its total deformation is decreased by 22.1%, indicating improved static performance.

Therefore, through parameter optimization, the mass of the A-axis support is reduced under the premise of ensuring static stiffness, and its static performance is enhanced.

(3) This research method holds certain theoretical and practical significance, providing valuable references for the design and manufacturing of machine tool A-axis supports.

REFERENCES

[1] Li Shuzhi. Thermal Analysis and Error Modeling of Double-Swing Angle Milling Heads Based on Hybrid Algorithm [D]. Hebei: Yanshan University, 2016: 1–2.

[2] Liang Cheng, Liu Jianqun. Current Status and Development Trends of Five-Axis CNC Machine Tool Technology [J]. Machinery Manufacturing, 2010, 48(01): 5–7.

[3] Zhang Kun, Wang Zemin, Chen Shijin. Research on Structural Design of High-Precision Swing Angle Milling Heads [J]. Mechanical Design and Manufacturing, 2011(06): 25–27.

[4] Zhang Di. Accuracy Analysis and Accuracy Retention Study of Direct-Drive A/C Axis Double-Swing Angle Milling Head [D]. Shenyang University of Technology, 2015.

[5] Liu Shihao. Research on Thermal–Force Coupling Dynamic Modeling Analysis and Optimization Methods for Gantry Machine Tool Feed Systems [D]. Jiangsu: Nanjing University of Aeronautics and Astronautics, 2013: 1–2.

[6] Zheng Peng, Yan Ming, Sun Shuxia, et al. Torsional Stiffness of Direct-Drive A/C Axis Double-Swing Angle Milling Head [J]. Medium and High-End CNC Machine Tools and Key Technologies, 2011, (8): 44–46.

[7] Wu Fenghe, Li Yongxin, Li Shuzhi, et al. Quantitative Allocation of Transmission Accuracy for Double-Swing Angle Milling Heads Based on Sensitivity Weighting [J]. China Mechanical Engineering, 2017, 28(22): 2675–2680.

[8] Zhu Chuanda. Geometric and Planar Cutting Force Error Modeling and Identification for Three-Axis CNC Machine Tools [D]. Tianjin University of Technology, 2025.000484.

[9] Yuan Guang. Principles of Metal Cutting and Cutting Tools [M]. Beijing: Mechanical Industry Press, 2006.

[10] Experimental Study on Milling Force Model of Aviation Aluminum Alloy 7050-T7451.

[11] Characteristic Analysis and Thermal Deformation Experimental Study of A/B Double-Swing Angle Milling Head, Li Rui.

[12] Zhang Song, Liu Bin, Fang Yujie. Research Progress in Lightweight Technology for CNC Machine Tools [J]. Aeronautical Manufacturing Technology, 2020, 63(14): 14–22.